RESEARCH ARTICLE

Activation of Sodium-Dependent Glutamate Transporters Regulates the Morphological Aspects of Oligodendrocyte Maturation via Signaling through Calcium/Calmodulin-Dependent Kinase IIβ's Actin-Binding/-Stabilizing Domain

Zila Martinez-Lozada,[1,2] Christopher T. Waggener,[1] Karam Kim,[3] Shiping Zou,[1] Pamela E. Knapp,[1] Yasunori Hayashi,[3,4] Arturo Ortega,[2] and Babette Fuss[1]

Signaling via the major excitatory amino acid glutamate has been implicated in the regulation of various aspects of the biology of oligodendrocytes, the myelinating cells of the central nervous system (CNS). In this respect, cells of the oligodendrocyte lineage have been described to express a variety of glutamate-responsive transmembrane proteins including sodium-dependent glutamate transporters. The latter have been well characterized to mediate glutamate clearance from the extracellular space. However, there is increasing evidence that they also mediate glutamate-induced intracellular signaling events. Our data presented here show that the activation of oligodendrocyte expressed sodium-dependent glutamate transporters, in particular GLT-1 and GLAST, promotes the morphological aspects of oligodendrocyte maturation. This effect was found to be associated with a transient increase in intracellular calcium levels and a transient phosphorylation event at the serine $(S)^{371}$ site of the calcium sensor calcium/calmodulin-dependent kinase type IIβ (CaMKIIβ). The potential regulatory S^{371} site is located within CaMKIIβ's previously defined actin-binding/-stabilizing domain, and phosphorylation events within this domain were identified in our studies as a requirement for sodium-dependent glutamate transporter-mediated promotion of oligodendrocyte maturation. Furthermore, our data provide good evidence for a role of these phosphorylation events in mediating detachment of CaMKIIβ from filamentous (F)-actin, and hence allowing a remodeling of the oligodendrocyte's actin cytoskeleton. Taken together with our recent findings, which demonstrated a crucial role of CaMKIIβ in regulating CNS myelination *in vivo*, our data strongly suggest that a sodium-dependent glutamate transporter–CaMKIIβ–actin cytoskeleton axis plays an important role in the regulation of oligodendrocyte maturation and CNS myelination.

GLIA 2014;62:1543–1558

Key words: myelin, calcium signaling, differentiation, central nervous system, actin cytoskeleton

Introduction

Glutamate (Glu), the major excitatory amino acid, mediates a wide variety of cellular responses in the developing and adult central nervous system (CNS) not only by affecting signal transduction in neurons but also by regulating glia cells, including the myelinating cells of the CNS, oligodendrocytes (Kolodziejczyk et al., 2010). Interestingly, the primary mode of Glu release affecting differentiating cells of

View this article online at wileyonlinelibrary.com. DOI: 10.1002/glia.22699

Published online May 27, 2014 in Wiley Online Library (wileyonlinelibrary.com). Received July 26, 2013, Accepted for publication May 9, 2014.

Address correspondence to Babette Fuss, Department of Anatomy and Neurobiology, Virginia Commonwealth University, PO Box 980709, Richmond, VA. E-mail: bfuss@vcu.edu

From the [1]Department of Anatomy and Neurobiology, Virginia Commonwealth University Medical Center, Richmond, Virginia; [2]Departamento de Toxicología, Centro de Investigación y de Estudios Avanzados del Instituto Politécnico Nacional, México D.F., México; [3]Brain Science Institute, RIKEN, Wako, Saitama, Japan; [4]Saitama University Brain Science Institute, Saitama University, Saitama, Japan.

*Zila Martinez-Lozada and Christopher T. Waggener contributed equally to this work.

Additional Supporting Information may be found in the online version of this article.

the oligodendrocyte lineage during development and under physiological conditions appears to be vesicle exocytosis along unmyelinated axons (Kukley et al., 2007; Ziskin et al., 2007) although release from electrically active axons by reversal of Glu uptake has also been proposed (Kriegler and Chiu, 1993). The prominent release of Glu from unmyelinated axons raises the possibility that Glu, in addition to mediating signaling events at synaptic junctions between axons and NG2-positive progenitor cells (De Biase et al., 2011; Etxeberria et al., 2010; Kukley et al., 2010), may be able to trigger cellular responses in differentiating oligodendrocytes that are involved in the regulation of oligodendrocyte maturation and CNS myelination.

Cells of the oligodendrocyte lineage have been described to express the members of all of the three major Glu-responsive transmembrane protein families (Kolodziejczyk et al., 2010; Matute, 2011). Out of these, metabotropic Glu receptors have been found downregulated as oligodendrocytes differentiate (Deng et al., 2004; Luyt et al., 2006). Ionotropic Glu receptors have primarily been associated with excitotoxicity (Matute, 2011) but they have also been implicated in the regulation of myelination (Lundgaard et al., 2013) and the preservation of neuronal integrity (Fruhbeis et al., 2013). Nevertheless, conditional deletion of the key receptor subunit of the NMDA subtype of iontropic Glu receptors in cells of the oligodendrocyte lineage was not found to lead to an apparent phenotype (De Biase et al., 2011; Guo et al., 2012). Thus, sodium-dependent Glu transporters emerge as good candidates for mediating Glu-evoked responses related to the maturation of differentiating oligodendrocytes. Of the known five mammalian sodium-dependent Glu transporters, also known as excitatory amino acid transporters (EAAT) or members of the solute carrier family 1 (SLC1), three have been found expressed by cells of the oligodendrocyte lineage, namely GLAST (EAAT1, SLC1A3), GLT-1 (EAAT2, SLC1A2), and EAAC1 (EAAT3, SLC1A1) (Arranz et al., 2008; DeSilva et al., 2009; Domercq and Matute, 1999; Kukley et al., 2010; Regan et al., 2007). Although these transporters have been well characterized to remove Glu from the extracellular environment (Beart and O'Shea, 2007; Danbolt, 2001), increasing evidence suggests that they play functional roles beyond extracellular Glu clearance (Flores-Mendez et al., 2013; Lopez-Colome et al., 2012; Martinez-Lozada et al., 2011).

Interestingly, signaling initiated by the activation of sodium-dependent Glu transporters has been proposed to activate calcium/calmodulin-dependent kinase type II (CaMKII) (Flores-Mendez et al., 2013; Martinez-Lozada et al., 2011), and one of the four CaMKII genes, namely CaMKIIβ, has recently been implicated in the regulation of oligodendrocyte maturation and CNS myelination (Waggener et al., 2013). More specifically, CaMKIIβ was implicated in promoting the morphological aspects of oligodendrocyte maturation, which are, to a large extent, regulated by the changes in the cellular cytoskeleton (Bauer et al., 2009), primarily via its actin-binding/-stabilizing domain rather than its well-known kinase catalytic domain. Thus, and based on the above observations, we investigated here a possible role of a sodium-dependent Glu transporter–CaMKIIβ–actin cytoskeleton axis in the regulation of the morphological aspects of oligodendrocyte maturation.

Materials and Methods

Animals

Sprague–Dawley female rats with early postnatal litters were obtained from Harlan Laboratories (Indianapolis, IN). All animal studies were approved by the Institutional Animal Care and Use Committee at Virginia Commonwealth University.

Antibodies

Supernatants from cultured hybridoma cells (clone A2B5; ATCC, Manassas, VA) were used for immunopanning. Anti-GLAST, anti-GLT-1, and anti-EAAC1 (Abcam, Cambridge, MA) antibodies were used for Western blot analysis as well as immunocytochemistry. Anti-CaMKII, anti-pCaMKII $T^{286/7}$ (Cell Signaling Technology, Danvers, MA), anti-pCaMKIIβ S^{371} (generated and characterized by us; Kim et al., in preparation), anti-GAPDH (EMD Millipore, Billerica, MA), and horseradish peroxidase (HRP)-labeled secondary antibodies (Vector Laboratories, Burlingame, CA) were used for Western blot analysis. Supernatants from cultured hybridoma cells (clone O4; gift from S.E. Pfeiffer), anti-myelin basic protein (MBP) antibodies (EMD Millipore, Billerica, MA), and Alexa 488- or Alexa 564-conjugated secondary antibodies (Life Technologies, Grand Island, NY) were used for immunocytochemistry.

Cell Culture

Primary rat oligodendrocyte progenitors were isolated from postnatal day 3 (P3) rat brains by A2B5 immunopanning (Barres et al., 1992; Lafrenaye and Fuss, 2011). Oligodendrocyte progenitors were either used directly in plasmid nucleofection experiments or plated onto fibronectin (10 μg/mL)-coated tissue culture dishes or glass coverslips. Plated oligodendrocyte progenitors were cultured in serum-free differentiation medium (Dulbecco's modified Eagle's medium [DMEM] containing 40 ng/mL tri-iodo-thyronine [T3; Sigma, St Louis, MO] and 1× N2 supplement [Life Technologies, Grand Island, NY]; DMEM/T3/N2). In siRNA-mediated gene silencing experiments, differentiating oligodendrocytes were transfected with siRNAs 24 h after plating. Otherwise, plated oligodendrocyte progenitors were allowed to differentiate for 48 h. Under these conditions, the majority of cells represented postmigratory, premyelinating oligodendrocytes as they expressed the O4 antigen (Sommer and Schachner, 1982; Warrington et al., 1993; data not shown). Such populations of differentiating oligodendrocytes were either directly analyzed or treated as indicated with the following compounds: L-Glu, D-aspartate (Asp), the competitive, nontransportable inhibitor

of sodium-dependent Glu transport DL-*threo*-β-benzyloxyaspartic acid (TBOA), the GLT-1-selective nontransportable inhibitor of Glu/Asp uptake dihydrokainic acid (DHK) (all from R&D Systems, Minneapolis, MN), the selective GLAST inhibitor UCPH-101 (Abcam, Cambridge, MA), the membrane permeable pharmacological inhibitor of CaMKII activity KN-93, or its inactive derivative KN-92 (EMD Millipore, Billerica, MA). In the case of dual treatments, inhibitors were added 30 min prior to the application of L-Glu or D-Asp. Cells were analyzed 6 h after the addition of L-Glu or D-Asp unless stated otherwise. Typically, at least three independent experiments were performed, whereby an independent experiment refers to an experiment in which cells were isolated from a separate P3 rat litter at an independent time point (day) and treated separately from all other independent experiments. In each experiment, triplicate coverslips (cultures) were prepared for all conditions/treatments.

Cells of the immortalized mouse oligodendroglial cell line CIMO were cultured in DMEM/5% fetal calf serum (FCS)/1 μg/mL interferon-γ (EMD Millipore, Billerica, MA) at 33°C (Bronstein et al., 1998) and then used in plasmid nucleofection experiments.

Quantitative (q)RT-PCR Analysis

For the determination of relative mRNA expression levels, qRT-PCR was performed on a CFX96 Real-Time PCR Detection System (Bio-Rad, Hercules, CA) using the iQ SYBR Green Supermix (Bio-Rad, Hercules, CA) and the following gene-specific primer pairs:

Glast: forward (5′-AGCCTGGGGTGTCTTCCACCA-3′), reverse (5′-ACCACAGCCTTGCACTTCAGTGTCT-3′);

Glt-1: forward (5′-TGGCGGCTCCCATCCACCCT-3′), reverse (5′-GGCGGCCGCTGGCTTTAGCA-3′);

Eaac1: forward (5′-GCCCACGAGCTCGGGATGCG-3′), reverse (5′-CACGATGCCCAGTACCACGGC-3′).

Ppia (reference gene): forward: (5′-GGAGACGAACCTGTAGGACG-3′) and reverse: (5′-GATGCTCTTTCCTCCTGTGC-3′)

Pgk1 (reference gene): forward: (5′-ATGCAAAGACTGGCCAAGCTAC-3′) and reverse: (5′-AGCCACAGCCTCAGCATATTTC-3′).

PCR conditions were as follows: 95°C for 3 min followed by 40 cycles of 95°C for 15 s, 58°C for 30 s, and 95°C for 10 s. For comparing the expression levels of the different genes, R_0 values were determined as described by Peirson et al. (2003). To determine the relative expression levels, the $\Delta\Delta C_T$ method was used (Livak and Schmittgen, 2001).

Western Blot Analysis

Cells were homogenized in lysis buffer (150 mM NaCl, 10 mM KCl, 20 mM HEPES [pH 7.0], 1 mM $MgCl_2$, 20% glycerol, and 1% Triton X-100) including the complete protease and phosphatase inhibitor cocktail (Thermo Scientific, Rockford, IL), and 12 μg (30 μg when using anti-GLAST antibodies) were used for Western blot analysis. Bound antibodies were detected using HRP-conjugated secondary antibodies in combination with the ECL Prime Western blotting detection reagent (GE Healthcare Life Sciences, Piscataway, NJ). Chemiluminescent signals were detected by the exposure of photographic film (Kodak BioMax MR, Eastman Kodak, Rochester, NY) and quantified by densitometry using the ImageJ software package (Abramoff et al., 2004).

Immunocytochemistry

For immunocytochemistry using O4 hybridoma supernatants, cells were fixed in 4% of paraformaldehyde/phosphate-buffered saline (PBS), nonspecific binding sites were blocked in 10% FCS/DMEM, and cells were incubated with the supernatant (1:1 diluted in 10% FCS/DMEM) overnight. For immunocytochemical detection of GLAST, GLT-1, EAAC1, or MBP, cells were fixed in 4% of paraformaldehyde/PBS and then permeabilized using 0.5% Triton X-100/0.4 M sucrose/PBS. Subsequently, cells were incubated for 30 min in 10% FCS/DMEM and then overnight with anti-GLAST, anti-GLT-1, anti-EAAC1 (Abcam, Cambridge, MA), or anti-MBP (SMI99; Covance, Princeton, NJ) antibodies. Primary antibodies were detected using Alexa 488- or Alexa 564-conjugated secondary antibodies (Life Technologies, Grand Island, NY) and nuclei were counterstained using Hoechst 33342 (EMD Millipore, Billerica, MA).

siRNA-Mediated Gene Silencing

Differentiating oligodendrocytes were transfected with ON-TARGET*plus* siRNA SMARTpools directed against rat *Glast*, *Glt-1*, or *Eaac1* (Thermo Fisher Scientific, Pittsburg, PA) using Lipofectamine 2000 (Life Technologies, Grand Island, NY). As control, an ON-TARGET*plus* nontargeting siRNA pool (Thermo Fisher Scientific, Pittsburg, PA) was used. Transfection medium containing siRNA–lipofectamine complexes was replaced with serum-free differentiation medium (DMEM/T3/N2) after 3 h and cells were cultured for an additional 72 h. Knockdown of gene expression was assessed by qRT-PCR and Western blot analysis.

Process Morphology Analysis

Oligodendrocyte morphology was analyzed and quantified as described previously in detail (Dennis et al., 2008). Briefly, oligodendrocytes were immunostained using O4 hybridoma cell supernatants and the images of approximately 30 cells were taken for each treatment group in each experiment ($n \geq 3$; i.e. at least 90 cells per condition) using an Olympus BX51 inverted fluorescent microscope (Olympus America, Center Valley, PA). Cells were chosen over the entire field of the coverslip by scanning from the upper left to the lower right. Only cells that displayed the features of a healthy cell (based on the nuclear stain and membrane appearance) and were without overlap with any neighboring cell were selected for analysis. IP Lab imaging software (BD Biosciences Bioimaging, Rockville, MD) was used to determine the network area (total area within the radius of the O4 immunopositive process network minus the cell body). For the bar graphs representing network area, the mean value for cells cultured under control conditions was calculated and set to 100%. Adjusted, that is normalized, values for all cells were then averaged for each experimental condition. For the generation of representative images, confocal laser scanning microscopy was used (Zeiss LSM 510 META NLO; Carl Zeiss Microscopy, LLC, Thornwood, NY). Images represent 2D maximum projections of stacks of 0.5 μm optical sections.

Cell Count Analysis

To determine the number of MBP immunopositive cells, images of four fields per coverslip were taken with a 20× objective using an Olympus BX51 fluorescence microscope equipped with an Olympus DP72 CCD camera (Olympus America, Center Valley, PA). Three coverslips per condition for each of three independent experiments were analyzed, and Hoechst 33342-positive nuclei as well as MBP immunopositive oligodendrocytes were counted using the Cell Counter plugin to the ImageJ software package (Abramoff et al., 2004).

Intracellular Calcium Measurement

The concentrations of intracellular calcium were determined in principal as described previously (Grynkiewicz et al., 1985). Briefly, differentiating oligodendrocytes were loaded with the calcium indicator fura-2 AM ester (2.5 μM) and pluronic F-127 (0.01%) (Life Technologies, Grand Island, NY) in differentiation medium for 30 min at 37°C. Cells were washed and incubated in differentiation medium for an additional 30 min at 37°C. Ratiometric calcium measurements were made at 340 and 380 nm of excitation and 510–520 nm of emission wavelengths with cells cultured in differentiation medium (unless mentioned otherwise) using a Zeiss Observer.Z1 microscope in combination with the Axio VisionRel 4.8 software package (Carl Zeiss Microscopy, LLC, Thornwood, NY). Measurements were taken from at least nine cells per treatment group and experiment and from three independent experiments (i.e., a total of 27 cells per treatment group) before and after the application of the indicated compounds. To calculate intracellular free calcium concentrations (in nM), a calibration curve (Calcium Calibration Buffer Kit, Life Technologies, Grand Island, NY) was used.

Plasmid Nucleofection

A2B5 immunopanned oligodendrocyte progenitors or CIMO cells were nucleofected (Lonza Cologne GmbH, Cologne, Germany) with the following constructs: a plasmid encoding eGFP–CaMKIIβ (Okamoto et al., 2004), a control plasmid encoding eGFP alone, and plasmids encoding eGFP–CaMKIIβ^{allA} or eGFP–CaMKIIβ^{allD} in which alanine or aspartic acid residues replace all serine/threonine residues located within the variable domain (amino acid, 317–396) (Kim et al., in preparation). All the above plasmids have the same plasmid backbone derived from the eukaryotic expression vector pEGFP-C1 (Clontech Laboratories, Mountain View, CA). It is also worth noting that the eGFP tag has been shown not to interfere with CaMKIIβ function (Okamoto et al., 2004, 2007).

To visualize F-actin in CIMO cells, cells were fixed in 4% paraformaldehyde/0.5% glutaraldehyde/0.4 M sucrose/PBS and then incubated with Acti-stain 555 phalloidin (Cytoskeleton, Denver, CO). Colocalization was quantified by determining weighted colocalization coefficients (Manders et al., 1993) using the ZEN software package (Carl Zeiss MicroImaging, LLC, Thornwood, NY) and dual-color confocal images of cellular protrusion that were imaged using a 63× objective and 2× digital zoom. At least 20 cells per condition and experiment were analyzed in three independent experiments (i.e., a total of at least 60 cells per condition).

To visualize F-actin in differentiating oligodendrocytes, a plasmid (pCAGGS backbone; Niwa et al., 1991) encoding Lifeact (Riedl et al., 2008) fused to mRuby (Kredel et al., 2009) was used. For the generation of representative images, confocal laser scanning microscopy was used (Zeiss LSM 510 META NLO; Carl Zeiss Microscopy, LLC, Thornwood, NY). Images represent 2D maximum projections of stacks of 0.5 μm optical sections.

Statistical Analysis

For statistical analysis, the GraphPad Prism software (GraphPad Software, La Jolla, CA) was used. In the case of two or more groups of data composed of variable values, two-tailed Student's *t*-tests or Kruskal–Wallis one-way analyses of variance (ANOVA) combined with Dunn's *post hoc* or Student–Newman–Keuls tests were performed. When comparing a single control group with experimental groups of data, ANOVA with Dunnett's *post hoc* tests was used. In the case data were compared with a set control value (1 or 100%) lacking variability, one-sample *t*-tests were used (Dalgaard, 2008; Skokal and Rohlf, 1995).

Results

Sodium-Dependent Glu Transport, Mediated Primarily by GLAST and GLT-1, Promotes the Morphological Maturation of Differentiating Oligodendrocytes

As introduced above, the sodium-dependent Glu transporter genes *Glast*, *Glt-1*, and *Eaac1* have been found to be expressed by cells of the oligodendrocyte lineage. To confirm such expression in differentiating oligodendrocytes in our culture system, qRT-PCR analysis was performed and revealed relative mRNA expression levels of *Glast* > *Glt-1* > *Eaac1* (Fig. 1A). Further validation was obtained through Western blot analysis and immunocytochemistry (Fig. 1B,C). Notably, in particular GLAST and GLT-1 were readily detectable not only in the cell body but also in the cellular processes.

To assess a potential role of sodium-dependent Glu transporters beyond extracellular Glu clearance, differentiating oligodendrocytes were treated with 100 μM of L-Glu and morphological aspects of oligodendrocyte maturation were assessed via a quantification of the network area as described previously in detail (Dennis et al., 2008). As shown in Fig. 2A–C, L-Glu treatment had a maturation-promoting effect that was seen as early as 2 h and up to 6 h. Importantly, this effect could be blocked by pretreatment with TBOA (Fig. 2A,B), a competitive and nontransportable inhibitor of sodium-dependent Glu transport (Shigeri et al., 2001; Shimamoto et al., 1998). In agreement with previous studies, no obvious effects on cell survival were noted in the presence of the L-Glu and TBOA concentrations used here and within the time frames analyzed (Deng et al., 2006 and data not shown).

To further substantiate that sodium-dependent Glu transporters play a predominant role in the observed maturation-promoting effect exerted by L-Glu, the naturally

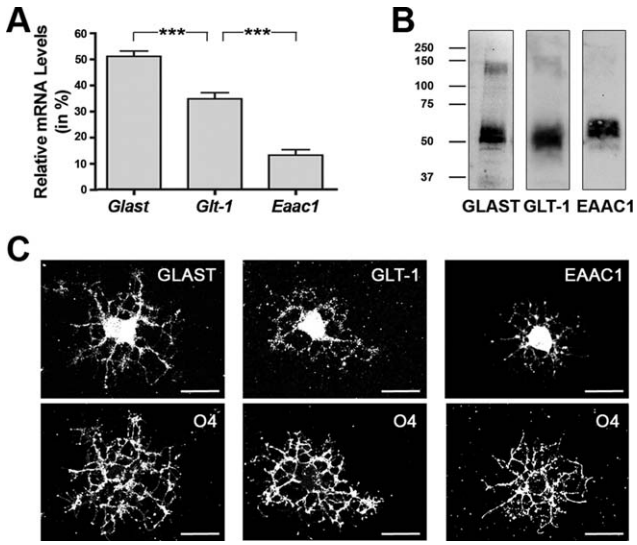

FIGURE 1: Sodium-dependent Glu transporters are expressed in differentiating oligodendrocytes. A: Bar graph representing sodium-dependent Glu transporter mRNA levels as determined by qRT-PCR analysis. Total Glu transporter mRNA levels (*Glast*+*Glt-1*+*Eaac1*) were set to 100% and the values for the individual gene-specific mRNA levels were adjusted accordingly. Data represent means ± SEM ($n = 3$ independent experiments, $^{***}P \leq 0.001$, ANOVA). B: Representative Western blots showing sodium-dependent Glu transporter protein expression. Numbers to the left indicate molecular weights in kDa. C: Representative images of differentiating oligodendrocytes double-immunostained using anti-GLAST, -GLT-1, or -EAAC1 antibodies in combination with O4 hybridoma supernatants. Scale bars: 20 μm.

occurring amino acid D-Asp was used as a Glu-equivalent agonist. Similar to L-Glu, D-Asp is efficiently taken up through the sodium-dependent Glu transporter system (Danbolt and Storm-Mathisen, 1986; Davies and Johnston, 1976; Kanai and Hediger, 1992; Palacin et al., 1998; Pines et al., 1992). In contrast to L-Glu, however, D-Asp does not activate non-NMDA receptor ionotropic and metabotropic Glu receptors (Domercq et al., 2005; Errico et al., 2008; Sugiyama et al., 1989), and it is not metabolized by glutamine synthetase (Bender et al., 1997). Thus, the use of D-Asp eliminates potential confounding effects that may be owing to an activation of AMPA/kainate and/or metabotropic Glu receptors and/or the release of glutamine via the sodium-dependent neutral amino acid transporter system. As shown in Fig. 2D, D-Asp elicited an effect on the oligodendrocyte process network that was comparable to the one seen upon treatment with L-Glu (compare Fig. 2B with 2D).

It has been well demonstrated that morphological maturation of oligodendrocytes occurs during development concurrently with changes in gene expression (Baumann and Pham-Dinh, 2001; Emery, 2010; Pfeiffer et al., 1993). Under experimental conditions, however, molecular mechanisms regulating cellular morphology may be uncoupled from those that regulate gene expression (Buttery and ffrench-Constant, 1999; Kim et al., 2006; Lafrenaye and Fuss, 2011; Osterhout et al., 1999; Waggener et al., 2013). Thus, and to assess a potential role of L-Glu and the activity of sodium-dependent Glu transporters on myelin gene expression, potential changes in *Mbp* expression were assayed using immunocytochemistry. In these experiments, no significant differences in the number of MBP-positive cells were noted (Fig. 2E,F), thus suggesting that the sodium-dependent Glu transporter-mediated effect on oligodendrocyte maturation is primarily associated with the morphological aspects of this process.

As shown in Fig. 1, differentiating oligodendrocytes express more than one of the known sodium-dependent Glu transporter genes. To evaluate the role of individual transporter genes, differentiating oligodendrocytes were transfected with siRNA pools specifically silencing *Glast*, *Glt-1*, or *Eaac1* expression. Knockdown of gene expression was confirmed by Western blot analysis, which revealed a specific reduction in transporter protein levels of at least 70% (Supp. Info. Fig. S1). Importantly, downregulation of a particular transporter gene was not associated with compensatory upregulation of any other transporter gene (Supp. Info. Fig. S1). In addition, no effect on the oligodendrocyte network area was noted upon knockdown of sodium-dependent Glu transporter expression alone (data not shown). However, knockdown of either *Glast* or *Glt-1* expression was found to eliminate the effect of L-Glu on the oligodendrocyte network area (Fig. 2G). For *Eaac1*, the sodium-dependent Glu transporter with much lower mRNA expression levels when compared with *Glast* or *Glt-1*, knockdown of gene expression was seen to only partially attenuate the effect of L-Glu on the oligodendrocyte network area (*siCtrl*+Glu: 157 ± 7%, *siEaac1* + Glu: 136 ± 6%, $P = 0.007$, ANOVA).

Taken together, the abovementioned data demonstrate that L-Glu can promote the morphological aspects of oligodendrocyte maturation via a sodium-dependent L-Glu transporter-mediated mechanism. In addition, they suggest that even a slight decline in the oligodendrocyte-derived expression of sodium-dependent L-Glu transporters can reduce the effect of L-Glu on the maturation of differentiating oligodendrocytes.

Activation of Sodium-Dependent Glu Transporters in Differentiating Oligodendrocytes Leads to a Transient Increase in Intracellular Calcium Levels

Having established that the activation of sodium-dependent Glu transporters promotes the morphological maturation of differentiating oligodendrocytes, we next wished to explore potential downstream signaling events involved in this process. These signaling-related studies were focused on calcium-mediated events as it had been previously demonstrated that Glu transport can activate the reverse mode of the

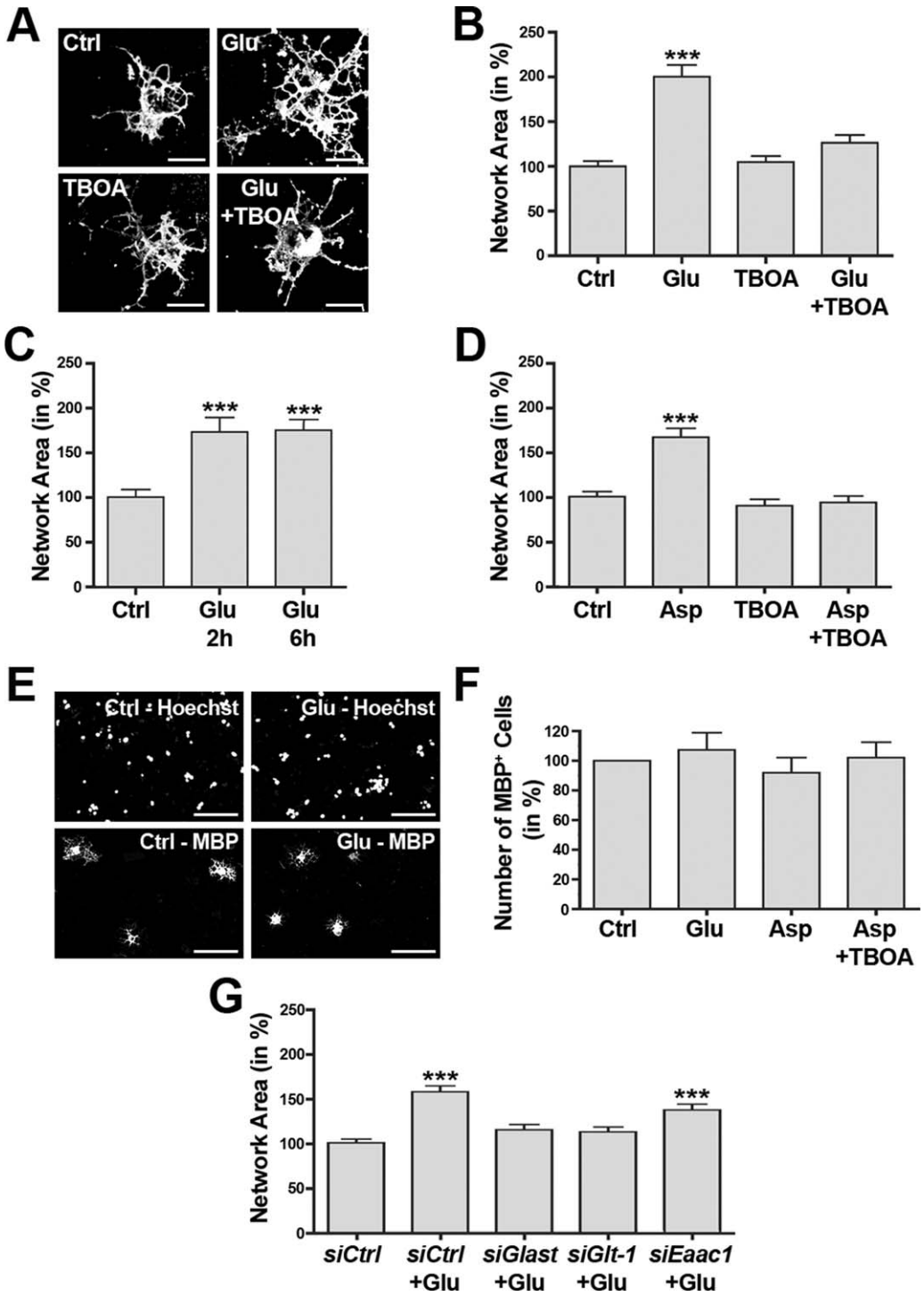

FIGURE 2: Activation of sodium-dependent Glu transporters promotes the morphological aspects of oligodendrocyte differentiation. **A–F**: Differentiating oligodendrocytes were treated for 6 h (unless noted otherwise) as indicated: control (Ctrl), L-Glu (100 μM), a nontransportable inhibitor of sodium-dependent Glu transport (TBOA, 100 μM), and D-Asp (100 μM). A: Representative images of differentiating oligodendrocytes immunostained using O4 hybridoma supernatants. Scale bars: 20 μm. B–D: Bar graphs representing quantitative analyses of oligodendrocyte network areas (Dennis et al., 2008). Data represent means ± SEM (***$P \leq 0.001$ compared with control, ANOVA). E: Representative images of differentiating oligodendrocytes stained with an antibody specific for MBP as well as with Hoechst 33342 (Hoechst) to visualize nuclei. Scale bars: 100 μm. F: Bar graph showing the number of MBP immunopositive cells normalized to the number of Hoechst-positive nuclei. Data represent means ± SEM. ANOVA revealed no statistically significant difference ($P \leq 0.05$). **G**: Bar graph showing oligodendrocyte network areas upon siRNA-mediated knockdown of individual sodium-dependent Glu transporters (as indicated) and subsequent treatment with L-Glu (100 μM). Data represent means ± SEM (***$P \leq 0.001$ compared with *siCtrl* nontreated, ANOVA).

sodium/calcium exchanger and hence lead to a transient increase in intracellular calcium levels (Lopez-Colome et al., 2012; Martinez-Lozada et al., 2011; Rojas et al., 2007). To assess the effect of an activation of sodium-dependent Glu transporters on intracellular calcium levels, D-Asp was used as a Glu-equivalent agonist, and the measurements of calcium were taken within the first minutes of the experiment, that is at an early stage of oligodendrocyte maturation. It is worth noting that the cells shown in Fig. 2A were imaged 6 h after Glu application, that is subsequent to a period of significant process outgrowth. As shown in Fig. 3, D-Asp treatment elicited a transient increase in intracellular calcium levels that appeared to occur first within cellular processes (Fig. 3A). This D-Asp-induced transient increase in free intracellular calcium levels was found to be dose dependent (Fig. 3B) and absent in the presence of TBOA (Fig. 3C). In addition, no such increase was observed in the absence of extracellular calcium (Fig. 3B).

To assess the functional contributions of each of the two main sodium-dependent Glu transporters expressed by differentiating oligodendrocytes, namely GLAST and GLT-1, DHK, a nontransportable inhibitor of L-Glu uptake selective for GLT-1 (Arriza et al., 1994), and UCPH-101, a nonsubstrate inhibitor selective for GLAST (Abrahamsen et al., 2013; Erichsen et al., 2010), were used. As shown in Fig. 3D, the D-Asp-mediated transient increase in intracellular calcium levels was completely abolished in the presence of DHK but only partially blocked in the presence of UCPH-101. Such a more prominent functional role of GLT-1 compared with GLAST in differentiating oligodendrocytes could be further validated by performing Glu uptake assays (data not shown).

Taken together, the abovementioned data support the idea that in differentiating oligodendrocytes L-Glu/D-Asp activates sodium-dependent Glu transporters and in particular GLT-1, which in turn mediates a transient increase in intracellular calcium levels via entry from the extracellular environment.

The Maturation-Promoting Effect of Sodium-Dependent Glu Transporters in Differentiating Oligodendrocytes is Mediated by a Transient Phosphorylation Event Within CaMKIIβ's Actin-Binding/-Stabilizing Domain

Our recent data provided good evidence for a critical role of the calcium sensor CaMKIIβ and in particular its actin-binding/-stabilizing domain in regulating oligodendrocyte maturation and CNS myelination (Waggener et al., 2013). Thus, CaMKIIβ and its actin-binding/-stabilizing domain may be directly involved in the sodium-dependent Glu transporter-mediated effect described here. Indeed, pretreatment of differentiating oligodendrocytes with KN-93, a membrane-permeable pharmacological inhibitor of CaMKIIβ's kinase catalytic as well as actin-binding/-stabilizing activity (Lin and Redmond, 2008; Sumi et al., 1991), was found to block the maturation-promoting effect of L-Glu on the oligodendrocyte process network (Fig. 4A). It is worth noting that KN-93 treatment alone and thus a continuous inhibition of CaMKII activity attenuated the morphological maturation of differentiating oligodendrocytes (Fig. 4A). This effect has been previously described and was found not to be associated with a change in cellular viability (Waggener et al., 2013).

To further assess the effect of L-Glu on CaMKII and in particular CaMKIIβ's actin-binding/-stabilizing domain in differentiating oligodendrocytes, phosphorylation events at CaMKII's $T^{286/7}$ and CaMKIIβ's S^{371} site were analyzed. CaMKII's $T^{286/7}$ site represents CaMKII's autophosphorylation site, which regulates autonomous CaMKII kinase catalytic activity and calcium-/calmodulin-binding affinity (Coultrap and Bayer, 2012). Owing to sequence conservation, phosphorylation events at this site could be detected only by pan pCaMKII $T^{286/7}$ antibodies. CaMKIIβ's S^{371} phosphorylation site is located within CaMKIIβ's unique actin-binding/-stabilizing domain (Kim et al., 2011; Lin and Redmond, 2009; Okamoto et al., 2007; O'Leary et al., 2006; Sanabria et al., 2009), and antibodies specifically recognizing this site have been generated by us. These antibodies were found not to recognize CaMKIIβ S^{371A}, a mutant form of CaMKIIβ that cannot be phosphorylated at its S^{371} site (data not shown). As shown in Fig. 4B,C, treatment of differentiating oligodendrocytes with L-Glu led to a significant increase in phosphorylation at CaMKIIβ's S^{371} site. This effect was time dependent and transient as an increase in phosphorylation was not seen prior to 30 min of treatment and beyond 4 h (Fig. 4C,F). No such increase in phosphorylation was observed at CaMKII's autophosphorylation ($T^{286/7}$) site within 15–60 min of L-Glu treatment (Fig. 4E), nor was a change in total protein levels of CaMKIIβ noted (Fig. 4D). Importantly, the effect of L-Glu on the phosphorylation at CaMKIIβ's S^{371} site could be blocked by pretreatment with TBOA (Fig. 4G).

To further assess the contribution of individual sodium-dependent Glu transporter genes in this L-Glu-mediated increase in pCaMKIIβ S^{371} levels, differentiating oligodendrocytes were transfected with siRNA pools specifically targeting *Glast*, *Glt-1*, or *Eaac1* expression. Similar to those observed for the effect of gene-specific knockdown of sodium-dependent Glu transporter expression on the oligodendrocyte network area (Fig. 2F), knockdown of *Glast* or *Glt-1* expression eliminated the effect of L-Glu on the phosphorylation of CaMKIIβ's S^{371} site, whereas the effect of a

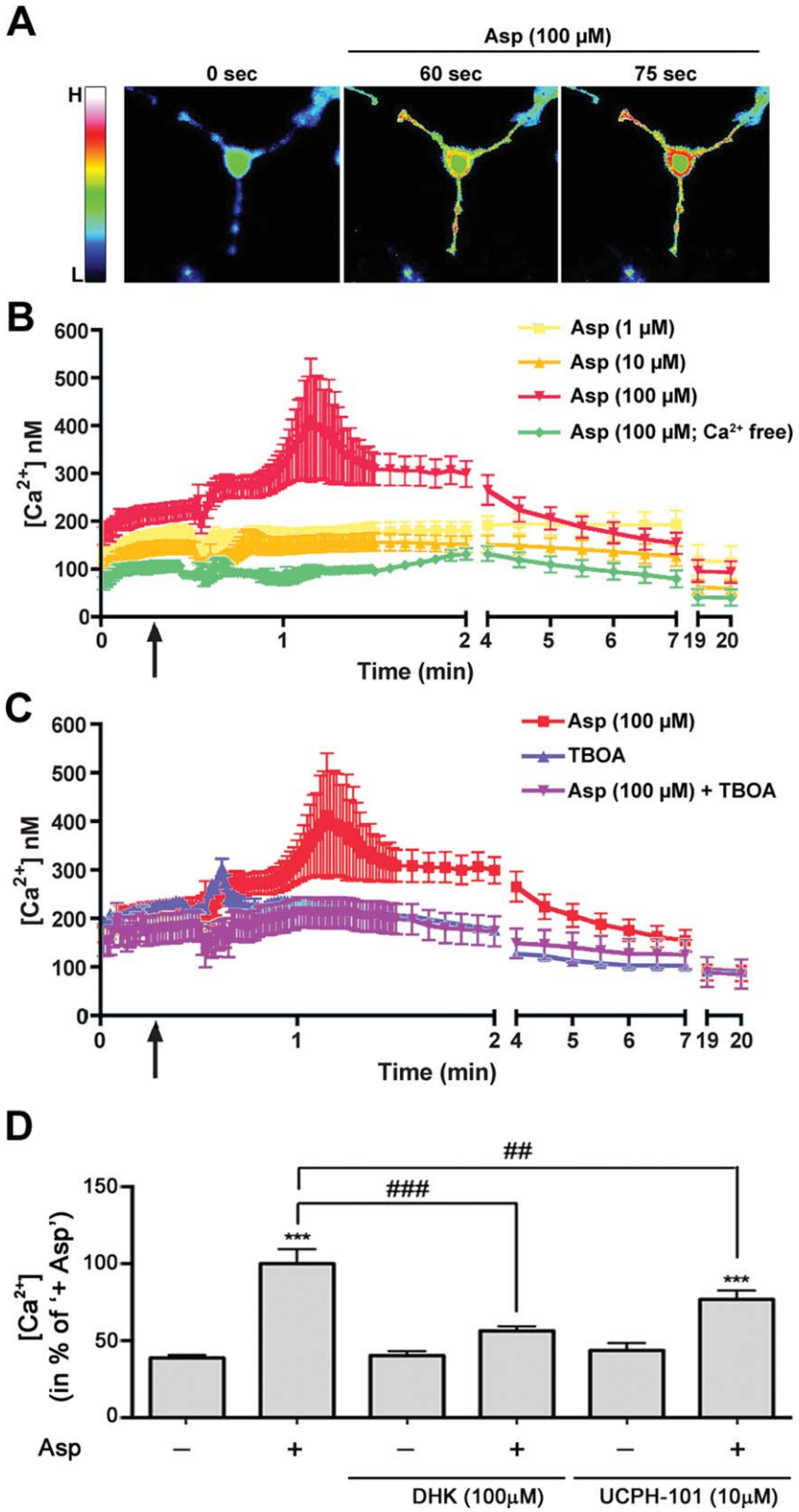

FIGURE 3: The activation of sodium-dependent Glu transporters increases intracellular calcium levels in the processes of early-stage differentiating oligodendrocytes. **A**: Representative pseudo-colored images of fura-2 AM fluorescence ratio measurements upon treatment with D-Asp. The bar to the left represents a relative color scale indicating low (L) and high (H) calcium levels. **B,C**: Time course of changes in free intracellular calcium concentrations [Ca^{2+}] upon different treatments as indicated in the inset shown in the upper right. Start of treatment is indicated by the arrow. The graphs represent means ± SEM. **D**: Bar graph showing a quantitative analysis of free intracellular calcium concentrations [Ca^{2+}] at the time point of highest response to D-Asp. The mean value for D-Asp-treated cells (+Asp) was set to 100% and the remaining values were calculated accordingly. Treatments are indicated along the *x*-axis. Data represent means ± SEM (***$P \leq 0.001$ compared with control [untreated], $^{###}P \leq 0.001$ and $^{##}P \leq 0.01$ compared with "+Asp," ANOVA).

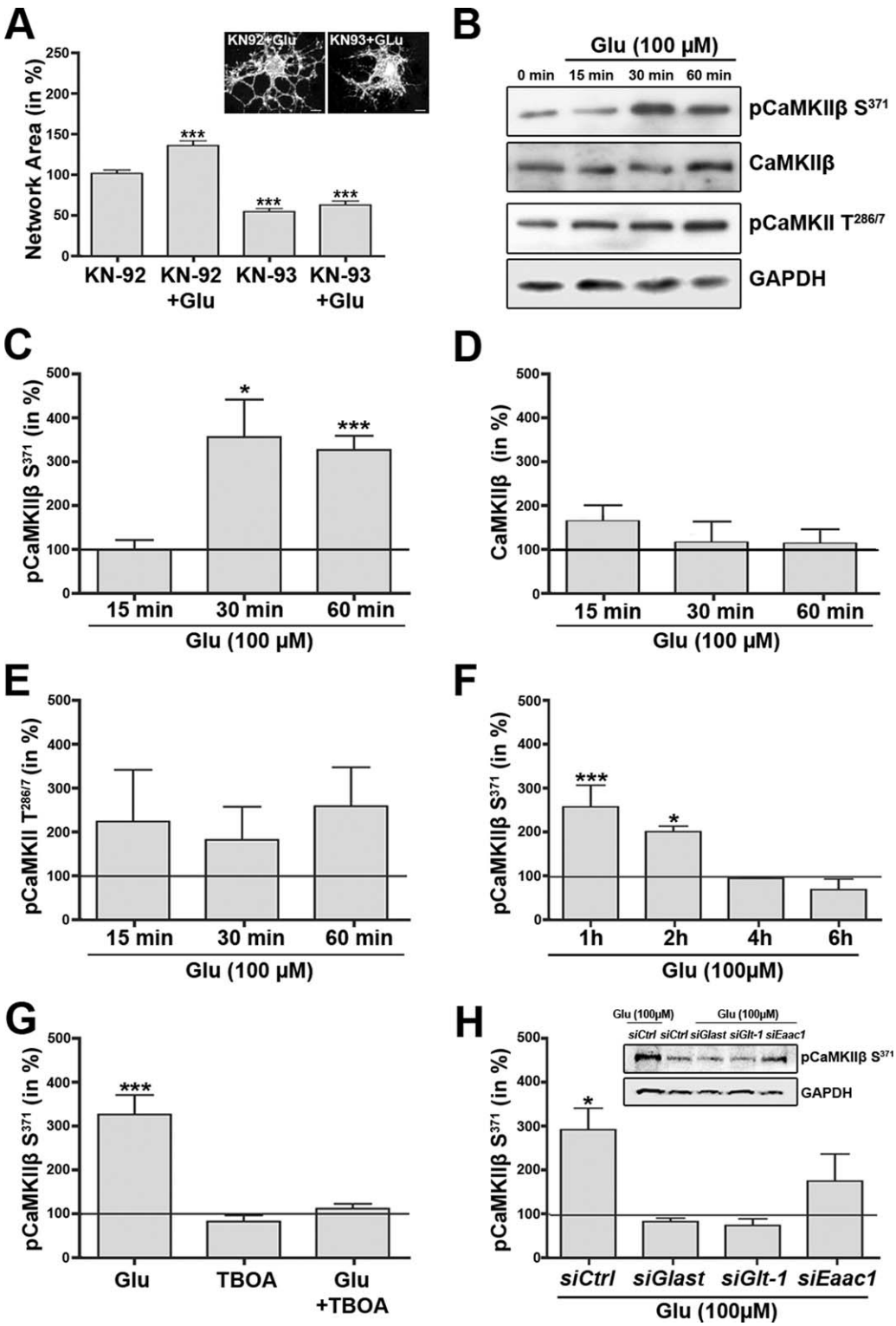

FIGURE 4: Activation of sodium-dependent Glu transporters leads to a transient phosphorylation event at CaMKIIβ's S^{371} site. **A**: Bar graph showing a quantitative analysis of the oligodendrocyte network area (Dennis et al., 2008). Cells were pretreated with the pharmacological CaMKII inhibitor KN-93 or its inactive derivative KN-92 and then incubated in the absence or presence (+Glu) of 100 µM of L-Glu. The mean values for control cells (pretreated with KN-92 and incubated in the absence of L-Glu) were set to 100% and the experimental values were calculated accordingly. Data represent means ± SEM (***$P \leq 0.001$ compared with control, ANOVA). The inset (upper right) shows representative images of differentiating oligodendrocytes treated with KN-92 plus L-Glu (left) or KN-93 plus L-Glu (right), and immunostained using O4 hybridoma supernatants. Scale bars: 5 µm. **B, inset in H**: Representative Western blots showing CaMKII phosphorylation (pCaMKIIβ S^{371}, pCaMKII $T^{286/7}$) or total CaMKIIβ protein levels. GAPDH protein levels are shown representatively for the Western blot for which anti-pCaMKII $T^{286/7}$ (B) or anti-pCaMKIIβ S^{371} (inset in H) antibodies were used. **C–H**: Bar graphs showing the levels of pCaMKIIβ S^{371} (C,F–H), total CaMKIIβ (D), or pCaMKII $T^{286/7}$ (E) at different time points after the addition of L-Glu (C–F), at the time point of 60 min after the addition of L-Glu and prior pretreatment with or without TBOA (G) or after transfection with siRNA pools as indicated and L-Glu treatment for 60 min (H). All CaMKII protein levels were normalized to GAPDH protein levels. The mean-normalized values for control (nontreated) cells were set to 100% (horizontal line) and the experimental values were calculated accordingly. Data represent means ± SEM of three independent experiments (***$P \leq 0.001$, *$P \leq 0.05$ compared with control, ANOVA).

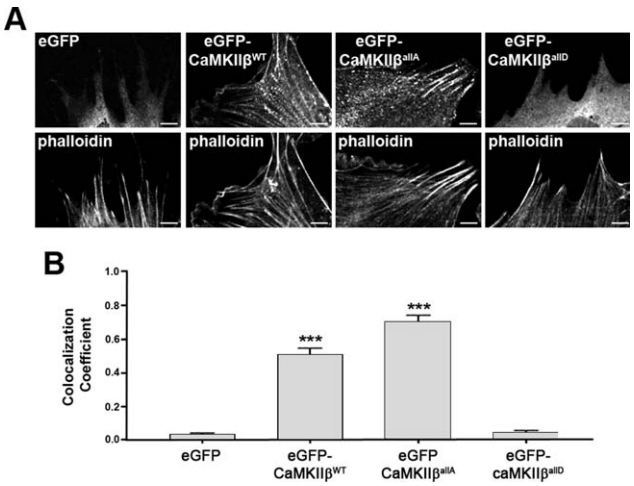

FIGURE 5: Phosphorylation events within CaMKIIβ's actin-binding/-stabilizing domain regulate the association of CaMKIIβ with F-actin. A: Representative images of CIMO cells nucleofected with plasmids encoding eGFP fusion proteins of CaMKIIβ (WT or mutant form as indicated) and stained for F-actin (phalloidin). Scale bars: 5 μm. B: Bar graph showing the weighted colocalization coefficients for eGFP fusion proteins and phalloidin. Data represent means ± SEM (*$P \leq 0.001$ compared with eGFP, ANOVA).**

knockdown of Eaac1 expression appeared less pronounced (Fig. 4H).

Our data described so far demonstrate that in differentiating oligodendrocytes, L-Glu can activate sodium-dependent Glu transporters, which in turn can mediate a transient increase in intracellular calcium levels, a transient phosphorylation event within CaMKIIβ's actin-binding/-stabilizing domain (S^{371} site) and a promotion of the morphological aspects of oligodendrocyte maturation.

Phosphorylation Events Within CaMKIIβ's Actin-Binding/-Stabilizing Domain Regulate the Association of CaMKIIβ with F-Actin and the Effect of L-Glu on the Oligodendrocyte Process Network

Our recent data, investigating the role of CaMKIIβ in the structural plasticity of dendritic spines, demonstrated that upon increases in intracellular calcium levels and serine (including S^{371})/threonine phosphorylation events within CaMKIIβ's actin-binding/-stabilizing domain CaMKIIβ detaches from F-actin (Kim et al., 2011). These data raised the possibility that sodium-dependent Glu transporter-mediated phosphorylation events within CaMKIIβ's actin-binding/-stabilizing domain may affect the oligodendrocyte process network via a change in CaMKIIβ's association with F-actin. To assess this idea, eGFP fusion proteins of CaMKIIβ mutant forms were generated in which the serine/threonine residues within the actin-binding/-stabilizing domain are either nonphosphorylatable (eGFP–$CaMKII\beta^{allA}$) or their phosphorylated state is mimicked (eGFP–$CaMKII\beta^{allD}$). In addition, eGFP–$CaMKII\beta^{WT}$ and eGFP–$CaMKII\beta^{K43R}$, a mutant that is impaired in ATP binding and thus inactive with regard to its kinase catalytic but not actin-binding activity (Okamoto et al., 2007), were used. To validate the proposed involvement of phosphorylation events within CaMKIIβ's actin-binding/-stabilizing domain on CaMKIIβ's association with F-actin, nucelofection studies were performed in cells of the oligodendroglial cell line CIMO. As shown in Fig. 5, nonphosphorylatable eGFP–$CaMKII\beta^{allA}$ as well as eGFP–$CaMKII\beta^{WT}$ largely colocalized with F-actin. In contrast, the phospho-mimetic eGFP–$CaMKII\beta^{allD}$ showed little colocalization with F-actin and appeared similar to eGFP distributed diffusely and throughout the cytoplasm.

Having established the F-actin-binding characteristics of the different forms of CaMKIIβ, we performed conucleofection experiments using a plasmid encoding Lifeact fused to mRuby in differentiating oligodendrocytes. Lifeact is a 17-amino-acid peptide, which binds to F-actin without interfering with actin organization and dynamics (Riedl et al., 2008) and thus allows reliable visualization of F-actin-rich structures. Using this approach, $CaMKII\beta^{allA}$ and eGFP–$CaMKII\beta^{WT}$ were readily detectable within F-actin-enriched regions located within cellular processes of differentiating oligodendrocytes (Fig. 6A, arrows). In contrast, eGFP–$CaMKII\beta^{allD}$ was similar to eGFP found predominantly localized to the cell body (Fig. 6A).

To further assess the role of the phosphorylation state of CaMKIIβ's actin-binding/-stabilizing domain and thus its level of association with F-actin in the L-Glu-mediated promotion of the morphological aspects of oligodendrocytes maturation, the effect of the expression of the different eGFP–CaMKIIβ forms on the oligodendrocyte network area was evaluated. As shown in Fig. 6B, the expression of nonphosphorylatable eGFP–$CaMKII\beta^{allA}$ blocked the maturation-promoting effect of L-Glu treatment. No such effect was observed when eGFP–$CaMKII\beta^{WT}$ or eGFP–$CaMKII\beta^{K43R}$ were expressed, suggesting that the L-Glu-mediated maturation-promoting effect may not require CaMKIIβ's kinase catalytic activity. Importantly and consistent with our previous findings (Waggener et al., 2013; Fig. 4A), constitutive expression of the phospho-mimetic eGFP–$CaMKII\beta^{allD}$ attenuated the morphological maturation of differentiating oligodendrocytes, likely owing to a dominant-negative effect with regard to F-actin binding. In addition, it eliminated the effect of L-Glu treatment on the oligodendrocyte process network.

Taken together, the abovementioned data support the idea that transient phosphorylation within CaMKIIβ's actin-binding/-stabilizing domain leading to transient detachment of CaMKIIβ from F-actin is a required step in the molecular mechanism that promotes the morphological aspects of

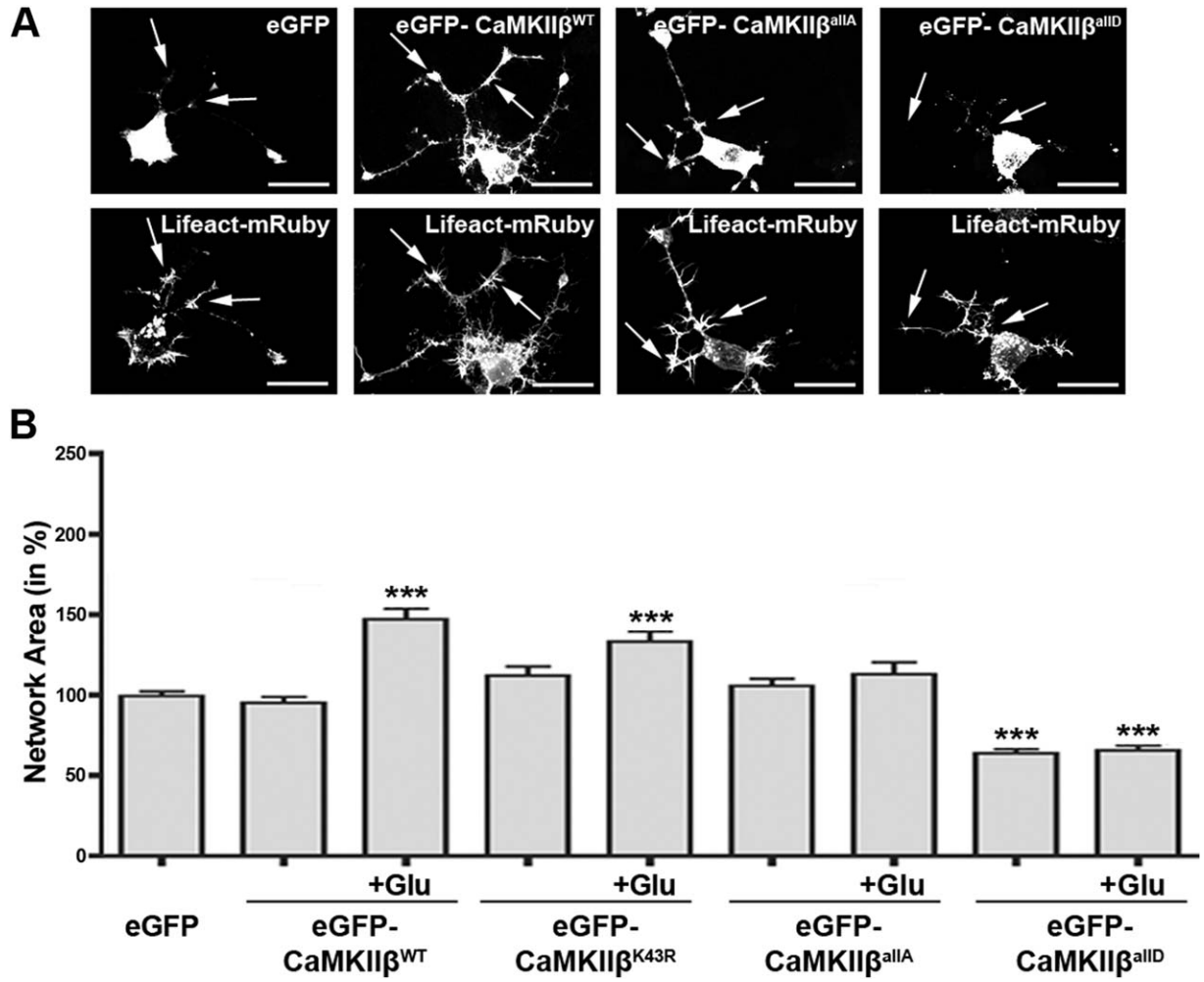

FIGURE 6: Phosphorylation events within CaMKIIβ's actin-binding/-stabilizing domain regulate the Glu-mediated promotion of the morphological aspects of oligodendrocyte maturation. A: Representative images of differentiating oligodendrocytes conucleofected with plasmids encoding an eGFP fusion protein of CaMKIIβ (WT or mutant form as indicated) and Lifeact–mRuby. Arrows point toward F-actin-enriched regions along cellular processes as visualized via Lifeact–mRuby fluorescence. Scale bars: 20 μm. B: Bar graph showing a quantitative analysis of the oligodendrocyte network area (Dennis et al., 2008). Cells were nucleofected as indicated and then incubated in the absence or presence (Glu) of 100 μM of L-Glu. The mean values for control cells (nucleofected with an eGFP-encoding plasmid and incubated in the absence of L-Glu) were set to 100% and the experimental values were calculated accordingly. Data represent means ± SEM (*$P \leq 0.001$ compared with control, ANOVA).**

oligodendrocyte maturation via an activation of sodium-dependent Glu transporters. Notably, constitutive (vs. transient) phosphorylation within CaMKIIβ's actin-binding/-stabilizing domain appears to have an opposing effect, that is to attenuate oligodendrocyte maturation.

Discussion

The studies described here investigated the role of sodium-dependent Glu transporters in the regulation of oligodendrocyte maturation. Based on the data presented and in combination with the ascribed function of CaMKIIβ's actin-binding/-stabilizing domain in the regulation of dendritic spine morphology (Okamoto et al., 2009), we propose the following model for the role of sodium-dependent Glu transporters in the regulation of oligodendrocyte maturation (Fig. 7). Under basal conditions, CaMKIIβ is, in differentiating oligodendrocytes, to a large extent, associated with the actin cytoskeleton. Glu release from, for example, unmyelinated axonal segments activates oligodendroglial sodium-dependent Glu transporters, which in turn activates the reverse mode of oligodendroglial sodium/calcium exchangers, resulting in a transient increase in intracellular calcium levels (Fig. 7A). This increase in intracellular calcium levels leads to phosphorylation events within CaMKIIβ's actin-binding/-stabilizing domain (including CaMKIIβ's S^{371} site), inactivation of CaMKIIβ's actin-binding activity and detachment of CaMKIIβ from the actin cytoskeleton. Such transient inactivation of CaMKIIβ's actin-binding activity opens a time window during which actin cytoskeleton remodeling events and actin polymerization are favored (Hoffman et al., 2013;

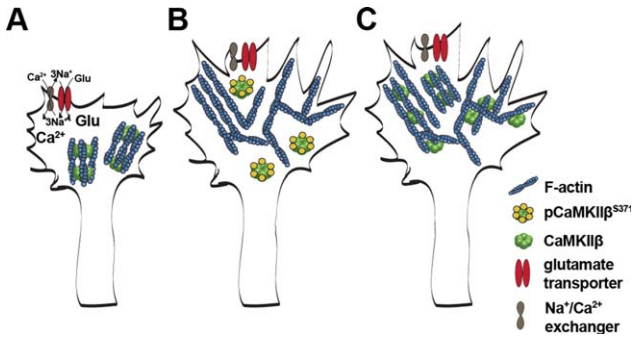

FIGURE 7: Proposed model for the role of a sodium-dependent Glu transporter-CaMKIIβ-actin cytoskeleton axis in the regulation of oligodendrocyte maturation. A: L-Glu **stimulates sodium-dependent Glu transporter activity, which in turn leads to an increase in intracellular sodium (Na^+) levels, activation of the reverse mode of the sodium/calcium exchanger, and a transient increase in intracellular calcium (Ca^{2+}) levels. B: The transient increase in intracellular calcium levels leads to phosphorylation events within CaMKIIβ's actin-binding/-stabilizing domain ($pCaMKII\beta^{S371}$), detachment of CaMKIIβ from F-actin, and the opening of a time window during which cytoskeletal rearrangements and morphological remodeling can occur. C: Upon deactivation (dephosphorylation), CaMKIIβ binds to F-actin and hence stabilizes the newly arranged cytoskeleton. Such cycles of activation and deactivation of CaMKIIβ's actin-binding activity allow reorganization of the actin cytoskeleton while at the same time preventing its uncontrolled disintegration. Adapted from Okamoto et al., Physiology, 2009, 24, 357–366.**

Okamoto et al., 2007; Sanabria et al., 2009) (Fig. 7B). This dynamic phase is followed by a phase of actin cytoskeleton stabilization via reactivation of CaMKIIβ's actin-binding activity through dephosphorylation (Fig. 7C). It is worth noting that the actin-binding activity of CaMKIIβ appears to be independent of its kinase catalytic activity, a concept that is supported by recent *in vitro* and *in vivo* studies (Borgesius et al., 2011; van Woerden et al., 2009). Interestingly, actin-binding properties have also been described for other members of the CaMKII gene family. These are, however, mediated by a structure–function domain different from the one identified in CaMKIIβ and analyzed here (Caran et al., 2001; Hoffman et al., 2013). Thus, further studies will be necessary to evaluate a potential contribution of CaMKII isozymes other than CaMKIIβ in the molecular mechanism described here. Importantly, and in contrast to its physiological role as proposed above, inactivation of CaMKIIβ's actin-binding properties in a constitutive (vs. transient) fashion appears to attenuate the morphological maturation of differentiating oligodendrocytes, an effect that is likely mediated by destabilization of the actin cytoskeleton over an extended period of time (Waggener et al., 2013). Thus, it is cycles of activation and deactivation of CaMKIIβ's actin-binding activity that allow reorganization of the actin cytoskeleton and a promotion of the morphological aspects of oligodendrocyte maturation. This idea is further supported by recent findings, demonstrating that balanced activation and deactivation of the actin filament severing and depolymerizing factor cofilin regulates the function of the myelinating cells of the peripheral nervous system, namely Schwann cells (Sparrow et al., 2012).

In addition to the abovementioned data, functional significance of oligodendroglial sodium-dependent Glu transporters for Glu uptake has been well demonstrated (Arranz et al., 2008; DeSilva et al., 2009; Domercq et al., 2005; Pitt et al., 2003; Regan et al., 2007). Consistent with our observations made when assessing calcium levels in differentiating oligodendrocytes upon treatment with D-Asp (Fig. 3), it has been shown that, at least in isolated optic nerve preparations, uptake of D-Asp occurs particularly within oligodendrocyte processes. This observation led to the idea that Glu homeostasis may be tightly regulated at the zones where axons and oligodendrocyte processes meet and in a fashion that may be analogous to what has been described for the tripartite synapse (Arranz et al., 2008). At the tripartite synapse, a so-called "Glu/glutamine shuttle" has been described (Martinez-Lozada et al., 2013; Rodriguez and Ortega, 2012; Uwechue et al., 2012) in which, upon its uptake, Glu is converted to glutamine by the enzymatic activity of glutamine synthetase. Glutamine is then released via sodium-dependent neutral amino acid transporters to be retaken up by neurons and to serve as a precursor for Glu synthesis. Glutamine synthetase is well known to be expressed by cells of the oligodendrocyte lineage (D'Amelio et al., 1990; Tansey et al., 1991; Warringa et al., 1988), and microarray studies indicate the expression of, in particular, the system *N*-amino acid transporter 2 (SNAT2 or SLC38A2) in differentiating oligodendrocytes (Cahoy et al., 2008). Nevertheless, more detailed studies will be necessary to clearly demonstrate that such a Glu/glutamine shuttle exists at axon–oligodendrocyte process interaction zones.

Our studies revealed a prominent expression of the sodium-dependent Glu transporter gene *Glast* in differentiating oligodendrocytes. This finding is in agreement with the previous observations made in tissue culture as well as *in vivo* in both rodents and humans (DeSilva et al., 2009; Domercq et al., 1999; Pitt et al., 2003; Regan et al., 2007; Vallejo-Illarramendi et al., 2006). In addition, a low-level expression of *Eaac1* is consistent with the reported presence of few *Eaac1*-positive cells in the developing optic nerve (Domercq et al., 1999). In contrast, the expression of *Glt-1* in cells of the oligodendrocyte lineage appears more complicated as it has *in vivo* and in rodents been described to be developmentally regulated and to be predominant at stages at which oligodendrocytes are premyelinating (Desilva et al., 2007; DeSilva et al., 2009; Domercq et al., 1999). However, in human tissue the expression of *Glt-1* has been reported to

occur in mature oligodendrocytes (Pitt et al., 2003; Werner et al., 2001). More importantly, our data suggest that on a functional level GLT-1 is the more prominent sodium-dependent Glu transporter in differentiating oligodendrocytes although GLAST also contributes to Glu-mediated uptake and transient increases in intracellular calcium levels. Such a predominant functional sodium-dependent Glu transporter role of GLT-1 in cells of the oligodendrocyte lineage is in agreement with previous findings made in rodents and humans (Pitt et al., 2003; Regan et al., 2007). However, a predominant role of EAAC1 in Glu uptake in maturing oligodendrocytes has also been described (DeSilva et al., 2009). Thus, additional studies will be necessary to more precisely define individual sodium-dependent Glu transporter contributions in cells of the oligodendrocyte lineage. Also, noteworthy is the finding that development in mice with single knockouts for *Glast*, *Glt-1*, or *Eaac1* occurs without apparent CNS gross phenotypes (Peghini et al., 1997; Tanaka et al., 1997; Watase et al., 1998), whereas double *Glast*/*Glt-1* knockout mice die *in utero* and show multiple developmental brain defects (Matsugami et al., 2006). These data indicate that during CNS development the loss of one sodium-dependent Glu transporter may be compensated for functionally by at least one of the remaining transporters, that is by a mechanism that could further complicate a delineation of individual roles for individual sodium-dependent Glu transporters.

Our model shown in Fig. 7 is suggestive of pivotal roles for oligodendroglial sodium/calcium exchangers and intracellular calcium levels in the regulation of oligodendrocyte maturation. This idea is supported by recent findings, implicating the sodium/calcium exchanger NCX3 in the regulation of oligodendrocyte differentiation (Boscia et al., 2012). In addition, process outgrowth has been found to be regulated by intracellular calcium levels in differentiating oligodendrocytes (Yoo et al., 1999). Interestingly, in our studies (Fig. 3), intracellular calcium levels remained slightly above the control levels after the initial rise. Such a calcium response is consistent with the previously described calcium responses mediated by signaling through sodium-dependent Glu transporters in astrocytes (Rojas et al., 2007). In the case of astrocytes, the initial rise in intracellular calcium concentration was found to be amplified by calcium release from ryanodine-sensitive calcium stores (Rojas et al., 2007), which are also expressed by cells of oligodendrocyte lineage (Simpson et al., 1998).

In the major demyelinating disease in human, multiple sclerosis (MS), a block in oligodendrocyte differentiation is considered one of the main causes of inefficient remyelination and repair (Chang et al., 2002; Fancy et al., 2010; Kremer et al., 2011; Kuhlmann et al., 2008). Interestingly, changes in sodium-dependent Glu transporter protein levels have been reported for white-matter areas surrounding MS lesions (Pitt et al., 2003; Vallejo-Illarramendi et al., 2006; Werner et al., 2001) and Glu levels have been found elevated in MS brains (Srinivasan et al., 2005; Trapp and Stys, 2009; Werner et al., 2001). Such changes in Glu homeostasis have been implicated in mediating excitotoxicity (Matute, 2011; Pitt et al., 2003). However, it has also been suggested that mature rodent as well as human oligodendrocytes are largely resistant to such Glu-mediated injury (Kolodziejczyk et al., 2009; Rosenberg et al., 2003; Wosik et al., 2004). Thus, and in light of our findings, it is tempting to speculate that the changes in Glu homeostasis and sodium-dependent Glu transporter signaling may primarily contribute to the differentiation block seen in MS rather than mediate oligodendrocyte cell death.

Acknowledgment

Grant sponsor: The NIH-NINDS.; Grant sponsor: NIH; Grant number: R01DA17310; Grant sponsor: Conacyt-Mexico.; Grant sponsor: Conacyt-Mexico.; Grant sponsor: Grant-in-Aid for Scientific Research and Grant-in-Aid for Scientific Research on the Innovative Area "Foundation of Synapse and Neurocircuit Pathology" from the Ministry of Education, Culture, Sports, Science, and Technology of Japan.; Grant sponsor: NIH-NINDS Center Core; Grant number: 5 P30 NS047463; Grant sponsors: Takeda Pharmaceuticals Co. Ltd.; Fujitsu Laboratories.

Microscopy was performed at the VCU Department of Anatomy and Neurobiology Microscopy Facility. Special thanks go to Steve Pfeiffer and Jeff Bronstein for providing the O4 hybridoma and CIMO cells, respectively.

References

Abrahamsen B, Schneider N, Erichsen MN, Huynh TH, Fahlke C, Bunch L, Jensen AA. 2013. Allosteric modulation of an excitatory amino acid transporter: The subtype-selective inhibitor UCPH-101 exerts sustained inhibition of EAAT1 through an intramonomeric site in the trimerization domain. J Neurosci 33:1068–1087.

Abramoff MD, Magelhaes PJ, Ram SJ. 2004. Image processing with ImageJ. Biophoton Int 11:36–42.

Arranz AM, Hussein A, Alix JJ, Perez-Cerda F, Allcock N, Matute C, Fern R. 2008. Functional glutamate transport in rodent optic nerve axons and glia. Glia 56:1353–1367.

Arriza JL, Fairman WA, Wadiche JI, Murdoch GH, Kavanaugh MP, Amara SG. 1994. Functional comparisons of three glutamate transporter subtypes cloned from human motor cortex. J Neurosci 14:5559–5569.

Barres BA, Hart IK, Coles HS, Burne JF, Voyvodic JT, Richardson WD, Raff MC. 1992. Cell death and control of cell survival in the oligodendrocyte lineage. Cell 70:31–46.

Bauer NG, Richter-Landsberg C, ffrench-Constant C. 2009. Role of the oligodendroglial cytoskeleton in differentiation and myelination. Glia 57: 1691–1705.

Baumann N, Pham-Dinh D. 2001. Biology of oligodendrocyte and myelin in the mammalian central nervous system. Physiol Rev 81:871–927.

Beart PM, O'Shea RD. 2007. Transporters for L-glutamate: An update on their molecular pharmacology and pathological involvement. Br J Pharmacol 150: 5–17.

Bender AS, Woodbury DM, White HS. 1997. The rapid L- and D-aspartate uptake in cultured astrocytes. Neurochem Res 22:721–726.

Borgesius NZ, van Woerden GM, Buitendijk GH, Keijzer N, Jaarsma D, Hoogenraad CC, Elgersma Y. 2011. BetaCaMKII plays a nonenzymatic role in hippocampal synaptic plasticity and learning by targeting alphaCaMKII to synapses. J Neurosci 31:10141–10148.

Boscia F, D'Avanzo C, Pannaccione A, Secondo A, Casamassa A, Formisano L, Guida N, Annunziato L. 2012. Silencing or knocking out the Na(+)/Ca(2+) exchanger-3 (NCX3) impairs oligodendrocyte differentiation. Cell Death Differ 19:562–572.

Bronstein JM, Hales TG, Tyndale RF, Charles AC. 1998. A conditionally immortalized glial cell line that expresses mature myelin proteins and functional GABA(A) receptors. J Neurochem 70:483–491.

Buttery PC, ffrench-Constant C. 1999. Laminin-2/integrin interactions enhance myelin membrane formation by oligodendrocytes. Mol Cell Neurosci 14:199–212.

Cahoy JD, Emery B, Kaushal A, Foo LC, Zamanian JL, Christopherson KS, Xing Y, Lubischer JL, Krieg PA, Krupenko SA, Thompson WJ, Barres BA. 2008. A transcriptome database for astrocytes, neurons, and oligodendrocytes: A new resource for understanding brain development and function. J Neurosci 28:264–278.

Caran N, Johnson LD, Jenkins KJ, Tombes RM. 2001. Cytosolic targeting domains of gamma and delta calmodulin-dependent protein kinase II. J Biol Chem 276:42514–42519.

Chang A, Tourtellotte WW, Rudick R, Trapp BD. 2002. Premyelinating oligodendrocytes in chronic lesions of multiple sclerosis. N Engl J Med 346:165–173.

Coultrap SJ, Bayer KU. 2012. CaMKII regulation in information processing and storage. Trends Neurosci 35:607–618.

Dalgaard P. 2008. Introductory Statistics with R. New York: Springer.

D'Amelio F, Eng LF, Gibbs MA. 1990. Glutamine synthetase immunoreactivity is present in oligodendroglia of various regions of the central nervous system. Glia 3:335–341.

Danbolt NC. 2001. Glutamate uptake. Prog Neurobiol 65:1–105.

Danbolt NC, Storm-Mathisen J. 1986. Na+-dependent "binding" of D-aspartate in brain membranes is largely due to uptake into membrane-bounded saccules. J Neurochem 47:819–824.

Davies LP, Johnston GA. 1976. Uptake and release of D- and L-aspartate by rat brain slices. J Neurochem 26:1007–1014.

De Biase LM, Kang SH, Baxi EG, Fukaya M, Pucak ML, Mishina M, Calabresi PA, Bergles DE. 2011. NMDA receptor signaling in oligodendrocyte progenitors is not required for oligodendrogenesis and myelination. J Neurosci 31: 12650–12662.

Deng W, Wang H, Rosenberg PA, Volpe JJ, Jensen FE. 2004. Role of metabotropic glutamate receptors in oligodendrocyte excitotoxicity and oxidative stress. Proc Natl Acad Sci USA 101:7751–7756.

Deng W, Yue Q, Rosenberg PA, Volpe JJ, Jensen FE. 2006. Oligodendrocyte excitotoxicity determined by local glutamate accumulation and mitochondrial function. J Neurochem 98:213–222.

Dennis J, White MA, Forrest AD, Yuelling LM, Nogaroli L, Afshari FS, Fox MA, Fuss B. 2008. Phosphodiesterase-Ialpha/autotaxin's MORFO domain regulates oligodendroglial process network formation and focal adhesion organization. Mol Cell Neurosci 37:412–424.

DeSilva TM, Kabakov AY, Goldhoff PE, Volpe JJ, Rosenberg PA. 2009. Regulation of glutamate transport in developing rat oligodendrocytes. J Neurosci 29:7898–7908.

Desilva TM, Kinney HC, Borenstein NS, Trachtenberg FL, Irwin N, Volpe JJ, Rosenberg PA. 2007. The glutamate transporter EAAT2 is transiently expressed in developing human cerebral white matter. J Comp Neurol 501: 879–890.

Domercq M, Etxebarria E, Perez-Samartin A, Matute C. 2005. Excitotoxic oligodendrocyte death and axonal damage induced by glutamate transporter inhibition. Glia 52:36–46.

Domercq M, Matute C. 1999. Expression of glutamate transporters in the adult bovine corpus callosum. Brain Res Mol Brain Res 67:296–302.

Domercq M, Sanchez-Gomez MV, Areso P, Matute C. 1999. Expression of glutamate transporters in rat optic nerve oligodendrocytes. Eur J Neurosci 11:2226–2236.

Emery B. 2010. Regulation of oligodendrocyte differentiation and myelination. Science 330:779–782.

Erichsen MN, Huynh TH, Abrahamsen B, Bastlund JF, Bundgaard C, Monrad O, Bekker-Jensen A, Nielsen CW, Frydenvang K, Jensen AA, Bunch L. 2010. Structure-activity relationship study of first selective inhibitor of excitatory amino acid transporter subtype 1: 2-Amino-4-(4-methoxyphenyl)−7-(naphthalen-1-yl)−5-oxo-5,6,7,8-tetrahydro-4H-chrom ene-3-carbonitrile (UCPH-101). J Med Chem 53:7180–7191.

Errico F, Rossi S, Napolitano F, Catuogno V, Topo E, Fisone G, D'Aniello A, Centonze D, Usiello A. 2008. D-aspartate prevents corticostriatal long-term depression and attenuates schizophrenia-like symptoms induced by amphetamine and MK-801. J Neurosci 28:10404–10414.

Etxeberria A, Mangin JM, Aguirre A, Gallo V. 2010. Adult-born SVZ progenitors receive transient synapses during remyelination in corpus callosum. Nat Neurosci 13:287–289.

Fancy SP, Kotter MR, Harrington EP, Huang JK, Zhao C, Rowitch DH, Franklin RJ. 2010. Overcoming remyelination failure in multiple sclerosis and other myelin disorders. Exp Neurol 225:18–23.

Flores-Mendez MA, Martinez-Lozada Z, Monroy HC, Hernandez-Kelly LC, Barrera I, Ortega A. 2013. Glutamate-dependent translational control in cultured Bergmann glia cells: eIF2alpha phosphorylation. Neurochem Res 38:1324–1332.

Fruhbeis C, Frohlich D, Kuo WP, Amphornrat J, Thilemann S, Saab AS, Kirchhoff F, Mobius W, Goebbels S, Nave KA, Schneider A, Simons M, Klugmann M, Trotter J, Krämer-Albers EM. 2013. Neurotransmitter-triggered transfer of exosomes mediates oligodendrocyte-neuron communication. PLoS Biol 11:e1001604.

Grynkiewicz G, Poenie M, Tsien RY. 1985. A new generation of Ca2+ indicators with greatly improved fluorescence properties. J Biol Chem 260:3440–3450.

Guo F, Maeda Y, Ko EM, Delgado M, Horiuchi M, Soulika A, Miers L, Burns T, Itoh T, Shen H, Lee E, Sohn J, Pleasure D. 2012. Disruption of NMDA receptors in oligodendroglial lineage cells does not alter their susceptibility to experimental autoimmune encephalomyelitis or their normal development. J Neurosci 32:639–645.

Hoffman L, Farley MM, Waxham MN. 2013. Calcium-calmodulin-dependent protein kinase II isoforms differentially impact the dynamics and structure of the actin cytoskeleton. Biochemistry 52:1198–1207.

Kanai Y, Hediger MA. 1992. Primary structure and functional characterization of a high-affinity glutamate transporter. Nature 360:467–471.

Kim HJ, DiBernardo AB, Sloane JA, Rasband MN, Solomon D, Kosaras B, Kwak SP, Vartanian TK. 2006. WAVE1 is required for oligodendrocyte morphogenesis and normal CNS myelination. J Neurosci 26:5849–5859.

Kim K, Hayashi M, Narayanan R, Suzuki A, Matsuura K, K. O, Hayashi Y. 2011. CaMKII gates rapid structural plasticity in hippocampal dendirtic spines. Program No 87207/E3 2011. Neuroscience Meeting Planner Washington, DC: Society for Neuroscience, Online.

Kolodziejczyk K, Hamilton NB, Wade A, Karadottir R, Attwell D. 2009. The effect of N-acetyl-aspartyl-glutamate and N-acetyl-aspartate on white matter oligodendrocytes. Brain 132:1496–1508.

Kolodziejczyk K, Saab AS, Nave KA, Attwell D. 2010. Why do oligodendrocyte lineage cells express glutamate receptors? F1000 Biol Rep 2:57.

Kredel S, Oswald F, Nienhaus K, Deuschle K, Rocker C, Wolff M, Heilker R, Nienhaus GU, Wiedenmann J. 2009. mRuby, a bright monomeric red fluorescent protein for labeling of subcellular structures. PLoS One 4:e4391.

Kremer D, Aktas O, Hartung HP, Kury P. 2011. The complex world of oligodendroglial differentiation inhibitors. Ann Neurol 69:602–618.

Kriegler S, Chiu SY. 1993. Calcium signaling of glial cells along mammalian axons. J Neurosci 13:4229–4245.

Kuhlmann T, Miron V, Cuo Q, Wegner C, Antel J, Bruck W. 2008. Differentiation block of oligodendroglial progenitor cells as a cause for remyelination failure in chronic multiple sclerosis. Brain 131:1749–1758.

Kukley M, Capetillo-Zarate E, Dietrich D. 2007. Vesicular glutamate release from axons in white matter. Nat Neurosci 10:311–320.

Kukley M, Nishiyama A, Dietrich D. 2010. The fate of synaptic input to NG2 glial cells: Neurons specifically downregulate transmitter release onto differentiating oligodendroglial cells. J Neurosci 30:8320–8331.

Lafrenaye AD, Fuss B. 2011. Focal adhesion kinase can play unique and opposing roles in regulating the morphology of differentiating oligodendrocytes. J Neurochem 115:269–282.

Lin YC, Redmond L. 2008. CaMKIIbeta binding to stable F-actin in vivo regulates F-actin filament stability. Proc Natl Acad Sci USA 105:15791–15796.

Lin YC, Redmond L. 2009. Neuronal CaMKII acts as a structural kinase. Commun Integr Biol 2:40–41.

Livak KJ, Schmittgen TD. 2001. Analysis of relative gene expression data using real-time quantitative PCR and the 2(-Delta Delta C(T)) method. Methods 25:402–408.

Lopez-Colome AM, Martinez-Lozada Z, Guillem AM, Lopez E, Ortega A. 2012. Glutamate transporter-dependent mTOR phosphorylation in Muller glia cells. ASN Neuro 4:e00095.

Lundgaard I, Luzhynskaya A, Stockley JH, Wang Z, Evans KA, Swire M, Volbracht K, Gautier HO, Franklin RJ, Attwell D, Káradóttir RT. 2013. Neuregulin and BDNF induce a switch to NMDA receptor-dependent myelination by oligodendrocytes. PLoS Biol 11:e1001743.

Luyt K, Varadi A, Durant CF, Molnar E. 2006. Oligodendroglial metabotropic glutamate receptors are developmentally regulated and involved in the prevention of apoptosis. J Neurochem 99:641–656.

Manders EMM, Verbeek FJ, Aten JA. 1993. Measurement of co-localization of objects in dualcolor confocal images. J Microsc 169:375–382.

Martinez-Lozada Z, Guillem AM, Flores-Mendez M, Hernandez-Kelly LC, Vela C, Meza E, Zepeda RC, Caba M, Rodriguez A, Ortega A. 2013. GLAST/EAAT1-induced glutamine release via SNAT3 in Bergmann glial cells: Evidence of a functional and physical coupling. J Neurochem 125:545–554.

Martinez-Lozada Z, Hernandez-Kelly LC, Aguilera J, Lopez-Bayghen E, Ortega A. 2011. Signaling through EAAT-1/GLAST in cultured Bergmann glia cells. Neurochem Int 59:871–879.

Matsugami TR, Tanemura K, Mieda M, Nakatomi R, Yamada K, Kondo T, Ogawa M, Obata K, Watanabe M, Hashikawa T, Tanaka K. 2006. From the cover: Indispensability of the glutamate transporters GLAST and GLT1 to brain development. Proc Natl Acad Sci USA 103:12161–12166.

Matute C. 2011. Glutamate and ATP signalling in white matter pathology. J Anat 219:53–64.

Niwa H, Yamamura K, Miyazaki J. 1991. Efficient selection for high-expression transfectants with a novel eukaryotic vector. Gene 108:193–199.

Okamoto K, Bosch M, Hayashi Y. 2009. The roles of CaMKII and F-actin in the structural plasticity of dendritic spines: A potential molecular identity of a synaptic tag? Physiology 24:357–366.

Okamoto K, Nagai T, Miyawaki A, Hayashi Y. 2004. Rapid and persistent modulation of actin dynamics regulates postsynaptic reorganization underlying bidirectional plasticity. Nat Neurosci 7:1104–1112.

Okamoto K, Narayanan R, Lee SH, Murata K, Hayashi Y. 2007. The role of CaMKII as an F-actin-bundling protein crucial for maintenance of dendritic spine structure. Proc Natl Acad Sci USA 104:6418–6423.

O'Leary H, Lasda E, Bayer KU. 2006. CaMKIIbeta association with the actin cytoskeleton is regulated by alternative splicing. Mol Biol Cell 17:4656–4665.

Osterhout DJ, Wolven A, Wolf RM, Resh MD, Chao MV. 1999. Morphological differentiation of oligodendrocytes requires activation of Fyn tyrosine kinase. J Cell Biol 145:1209–1218.

Palacin M, Estevez R, Bertran J, Zorzano A. 1998. Molecular biology of mammalian plasma membrane amino acid transporters. Physiol Rev 78:969–1054.

Peghini P, Janzen J, Stoffel W. 1997. Glutamate transporter EAAC-1-deficient mice develop dicarboxylic aminoaciduria and behavioral abnormalities but no neurodegeneration. EMBO J 16:3822–3832.

Peirson SN, Butler JN, Foster RG. 2003. Experimental validation of novel and conventional approaches to quantitative real-time PCR data analysis. Nucleic Acids Res 31:e73.

Pfeiffer SE, Warrington AE, Bansal R. 1993. The oligodendrocyte and its many cellular processes. Trends Cell Biol 3:191–197.

Pines G, Danbolt NC, Bjoras M, Zhang Y, Bendahan A, Eide L, Koepsell H, Storm-Mathisen J, Seeberg E, Kanner BI. 1992. Cloning and expression of a rat brain L-glutamate transporter. Nature 360:464–467.

Pitt D, Nagelmeier IE, Wilson HC, Raine CS. 2003. Glutamate uptake by oligodendrocytes: Implications for excitotoxicity in multiple sclerosis. Neurology 61:1113–1120.

Regan MR, Huang YH, Kim YS, Dykes-Hoberg MI, Jin L, Watkins AM, Bergles DE, Rothstein JD. 2007. Variations in promoter activity reveal a differential expression and physiology of glutamate transporters by glia in the developing and mature CNS. J Neurosci 27:6607–6619.

Riedl J, Crevenna AH, Kessenbrock K, Yu JH, Neukirchen D, Bista M, Bradke F, Jenne D, Holak TA, Werb Z, Sixt M, Wedlich-Soldner R. 2008. Lifeact: A versatile marker to visualize F-actin. Nat Methods 5:605–607.

Rodriguez A, Ortega A. 2012. The glia connection of the glutamate/glutamine shuttle. Am J Neurosci 3:32–38.

Rojas H, Colina C, Ramos M, Benaim G, Jaffe EH, Caputo C, DiPolo R. 2007. Na+ entry via glutamate transporter activates the reverse Na+/Ca2+ exchange and triggers Ca(i)2+-induced Ca2+ release in rat cerebellar Type-1 astrocytes. J Neurochem 100:1188–1202.

Rosenberg PA, Dai W, Gan XD, Ali S, Fu J, Back SA, Sanchez RM, Segal MM, Follett PL, Jensen FE, Volpe JJ. 2003. Mature myelin basic protein-expressing oligodendrocytes are insensitive to kainate toxicity. J Neurosci Res 71:237–245.

Sanabria H, Swulius MT, Kolodziej SJ, Liu J, Waxham MN. 2009. {beta}CaMKII regulates actin assembly and structure. J Biol Chem 284:9770–9780.

Shigeri Y, Shimamoto K, Yasuda-Kamatani Y, Seal RP, Yumoto N, Nakajima T, Amara SG. 2001. Effects of threo-beta-hydroxyaspartate derivatives on excitatory amino acid transporters (EAAT4 and EAAT5). J Neurochem 79:297–302.

Shimamoto K, Lebrun B, Yasuda-Kamatani Y, Sakaitani M, Shigeri Y, Yumoto N, Nakajima T. 1998. DL-threo-beta-benzyloxyaspartate, a potent blocker of excitatory amino acid transporters. Mol Pharmacol 53:195–201.

Simpson PB, Holtzclaw LA, Langley DB, Russell JT. 1998. Characterization of ryanodine receptors in oligodendrocytes, type 2 astrocytes, and O-2A progenitors. J Neurosci Res 52:468–482.

Skokal RR, Rohlf FJ. 1995. Biometry: The principle and practice in biological research. New York: W. H. Freeman and Company.

Sommer I, Schachner M. 1982. Cell that are O4 antigen-positive and O1 antigen-negative differentiate into O1 antigen-positive oligodendrocytes. Neurosci Lett 29:183–188.

Sparrow N, Manetti ME, Bott M, Fabianac T, Petrilli A, Bates ML, Bunge MB, Lambert S, Fernandez-Valle C. 2012. The actin-severing protein cofilin is downstream of neuregulin signaling and is essential for Schwann cell myelination. J Neurosci 32:5284–5297.

Srinivasan R, Sailasuta N, Hurd R, Nelson S, Pelletier D. 2005. Evidence of elevated glutamate in multiple sclerosis using magnetic resonance spectroscopy at 3 T. Brain 128:1016–1025.

Sugiyama H, Ito I, Watanabe M. 1989. Glutamate receptor subtypes may be classified into two major categories: A study on Xenopus oocytes injected with rat brain mRNA. Neuron 3:129–132.

Sumi M, Kiuchi K, Ishikawa T, Ishii A, Hagiwara M, Nagatsu T, Hidaka H. 1991. The newly synthesized selective Ca2+/calmodulin dependent protein

kinase II inhibitor KN-93 reduces dopamine contents in PC12h cells. Biochem Biophys Res Commun 181:968–975.

Tanaka K, Watase K, Manabe T, Yamada K, Watanabe M, Takahashi K, Iwama H, Nishikawa T, Ichihara N, Kikuchi T, Okuyama S, Kawashima N, Hori S, Takimoto M, Wada K. 1997. Epilepsy and exacerbation of brain injury in mice lacking the glutamate transporter GLT-1. Science 276:1699–1702.

Tansey FA, Farooq M, Cammer W. 1991. Glutamine synthetase in oligodendrocytes and astrocytes: New biochemical and immunocytochemical evidence. J Neurochem 56:266–272.

Trapp BD, Stys PK. 2009. Virtual hypoxia and chronic necrosis of demyelinated axons in multiple sclerosis. Lancet Neurol 8:280–291.

Uwechue NM, Marx MC, Chevy Q, Billups B. 2012. Activation of glutamate transport evokes rapid glutamine release from perisynaptic astrocytes. J Physiol 590:2317–2331.

Vallejo-Illarramendi A, Domercq M, Perez-Cerda F, Ravid R, Matute C. 2006. Increased expression and function of glutamate transporters in multiple sclerosis. Neurobiol Dis 21:154–164.

van Woerden GM, Hoebeek FE, Gao Z, Nagaraja RY, Hoogenraad CC, Kushner SA, Hansel C, De Zeeuw CI, Elgersma Y. 2009. BetaCaMKII controls the direction of plasticity at parallel fiber-Purkinje cell synapses. Nat Neurosci 12:823–825.

Waggener CT, Dupree JL, Elgersma Y, Fuss B. 2013. CaMKIIbeta regulates oligodendrocyte maturation and CNS myelination. J Neurosci 33:10453–10458.

Warringa RA, van Berlo MF, Klein W, Lopes-Cardozo M. 1988. Cellular location of glutamine synthetase and lactate dehydrogenase in oligodendrocyte-enriched cultures from rat brain. J Neurochem 50:1461–1468.

Warrington AE, Barbarese E, Pfeiffer SE. 1993. Differential myelinogenic capacity of specific developmental stages of the oligodendrocyte lineage upon transplantation into hypomyelinating hosts. J Neurosci Res 34:1–13.

Watase K, Hashimoto K, Kano M, Yamada K, Watanabe M, Inoue Y, Okuyama S, Sakagawa T, Ogawa S, Kawashima N, Hori S, Takimoto M, Wada K, Tanaka K. 1998. Motor discoordination and increased susceptibility to cerebellar injury in GLAST mutant mice. Eur J Neurosci 10:976–988.

Werner P, Pitt D, Raine CS. 2001. Multiple sclerosis: Altered glutamate homeostasis in lesions correlates with oligodendrocyte and axonal damage. Ann Neurol 50:169–180.

Wosik K, Ruffini F, Almazan G, Olivier A, Nalbantoglu J, Antel JP. 2004. Resistance of human adult oligodendrocytes to AMPA/kainate receptor-mediated glutamate injury. Brain 127:2636–2648.

Yoo AS, Krieger C, Kim SU. 1999. Process extension and intracellular Ca2+ in cultured murine oligodendrocytes. Brain Res 827:19–27.

Ziskin JL, Nishiyama A, Rubio M, Fukaya M, Bergles DE. 2007. Vesicular release of glutamate from unmyelinated axons in white matter. Nat Neurosci 10:321–330.